Polarizability of the Iodide Ion in Crystal

Elena Bichoutskaia* and Nicholas C. Pyper

University Chemical Laboratory, Lensfield Road, Cambridge, CB2 1EW United Kingdom

Received: December 1, 2006; In Final Form: April 16, 2007

The electronic dipole polarizability of the iodide ion in solid cubic NaI and KI is derived from ab initio electronic structure computations as function of closest cation−anion separation for the four-coordinated zinc blende structure, the 6-fold coordinated rock salt structure, and the 8-fold coordinated phase having the CsCl structure. The contributions from electron correlation were computed using Moller−Plessett perturbation theory taken to the second order. For both NaI and KI, the anion polarizability predicted for the observed rock-salt polymorph at the equilibrium separation agrees well with the value deduced from experiment. The anion polarizabilities increase with both decreasing coordination number at constant distance and with increasing distance at constant coordination number. Both the polarizabilities and their contributions from electron correlation are suppressed in-crystal relative to those computed for the free iodide ion. The ab initio predictions for the derivatives of the anion polarizabilities with respect to closest cation−anion separation are slightly smaller than those deduced from the experimental observations. Reviews of both the latter and the dipole polarizability derivatives previously computed for other alkali halides are presented. The distance dependence of the polarizability of the iodide ion in the point charge representation of the rock-salt lattice, computed ab initio, differs in shape slightly but significantly from that for either NaI or KI. This difference prevents the in-crystal polarizabilities and their distance derivatives from being predicted by shifting the point lattice polarizability function as previously shown to be possible for the salts of the lighter halides. The applicability of the light scattering model description of anion polarizabilities in condensed phases is investigated.

1. Introduction

There is much experimental and theoretical evidence, reviewed elsewhere,[1,2] that many crystals are essentially fully ionic. This provides the justification for theories which describe such crystals in terms of individual ions, which, although interacting, possess clearly identifiable individual properties. One of these properties, namely, the static electronic polarizabilities of ions in crystal is important for three broad classes of reason. First, they control, through their sum, the molar polarizability, the macroscopic dielectric response of ionic crystals as manifested by their refractive indices and high-frequency dielectric constants.[3,4] Furthermore, the close relationship between the polarizability and dielectric constant yields the condition, suggested by Herzfeld,[5] for determining the volume and hence pressure required to induce an insulator to metal transition. The utility of this condition is now well established for both elements and two component systems.[6,7] The second reason for the importance of individual ion polarizabilities is that they are intimately linked with the dipole−dipole dispersion coefficients. These coefficients, which govern the leading term in the van der Waals attraction between two ions, are given exactly by the Casimir−Polder type integral of the product of the imaginary frequency polarizabilities of the two ions.[8,9] Furthermore, the Slater−Kirkwood formula,[10] which requires only the much more readily available static electronic polarizabilities, emerges[11] as a two point Pade approximate to the Casimir−Polder type expression. It is now well-established that these dispersive attractions play an important role in determining both the overall cohesive properties of ionic crystals[3,12−15] as well the relative energies of different polymorphs of the same material.[3,12,16−18] The third reason for the importance of ion polarizabilities is that, in governing the response to static electric fields, they determine the charge-induced dipole energies, which arise when ions reside on sites of low symmetry. These interactions not only lower significantly the energies of defect formation in perfect crystals of high symmetry[19−20] but also are a crucial factor in explaining[2,21] within a fully ionic model, the structures of crystals whose low symmetries had previously been taken as evidence for significant covalency.

Despite the significance of ion polarizabilities, the literature up to the beginning of the 1980s not only contained a wide range of values for the polarizability of any individual ion but also gave no guidance about their reliability. However, in the 1980s, a series of ab initio electronic structure quantum chemistry computations of the polarizabilities of ions in a variety of accurate model descriptions of their environments in-crystal provided accurate and trustworthy values for a relatively small but significant number of ions.[22−24] The physical insights afforded by these computations provided the key for constructing a well-based empirical model, which enabled trustworthy values for the polarizabilities of many other ions to be deduced.[25] For the rubidium cation, the polarizability thereby deduced[25] was subsequently confirmed[26] by ab initio computations. The computations[22−24] and model[25] showed that the polarizabilities of cations having s^2 or p^6 outermost electronic configurations were essentially independent of their environment in-crystal, being the same as those of the free ions. Such computations also revealed that the polarizabilities of anions in-crystal were

* To whom correspondence should be addressed.

10.1021/jp068257s CCC: $37.00
Published on Web 06/05/2007

not only significantly reduced compared with those of the corresponding free anions[22,23,26,27] but also that the in-crystal values were not constant but depended on both the internuclear distance[28,29] and polymorph[29,30] in any one crystal. Furthermore, in comparisons of anion polarizabilities in different materials all at their respective equilibrium geometries, the polarizability of each anion depends on the counter cation.[22−25] For ions, such as halides, which, unlike the doubly charged oxide ion, are stable in the free state, the dependence of the anion polarizability on separation in any polymorph of any crystal was shown to exhibit a sigmoid dependence on the internuclear distance with the polarizability at large separation tending to that of the free anion.[29,31]

The ab initio quantum chemistry studies have provided a wealth of valuable data for fluorides, chlorides, and bromides[22,23,27,29−30] as well as for the oxide[25,28,29] and even the sulfide ion.[31] However, it is notable that, since none of these studies investigated the iodide ion, knowledge of its polarizability has been restricted to more empirical approaches. Thus, currently the must trustworthy values for the iodide polarizability were deduced by subtracting from the experimental molar polarizabilities of the alkali iodides reliable values of the cation polarizabilities taken either from ab initio computations or deduced from experimental data for salts of the lighter halogens.[25]

The first of the three objectives of this paper is to present an ab initio study of the polarizability of the iodide ion in three different cubic polymorphs of its sodium and potassium salts. The results provide a valuable check on the validity of the ionic description of these salts at least so far as concerns their electrical properties intimately connected with polarizabilities. The second objective is to use the resulting data to investigate further the overall conceptual models, which have been developed[29,32,33] with the aim of producing an overarching framework of the physical understanding of the behavior of this important property, both in a variety of different environments and in terms of the relationship between the polarizabilities of different anions. The third objective, achieved as a byproduct of the first, is to derive, for the in-crystal iodide ion, a trustworthy basis set, which could be used in further studies of this anion when it resides in sites of lower symmetry in which static ion-induced dipole interactions must be considered. Such knowledge will be valuable in any subsequent ab initio theoretical investigations of the structures and properties of small alkali halides encapsulated in carbon nanotubes, a topic of much current experimental[34−39] and theoretical[40−43] interest. A wealth of experimental data for encapsulated salts, both alkali halides as well as other less ionic materials, has recently become available from the application of newly developed methods in electron microscopy.[44,45] Knowledge of a good iodide basis set, capable of reproducing the ion-induced-dipole energies by virtue of its proven ability to describe the iodide polarizability, is particularly valuable for any ab initio theoretical studies because it is for encapsulated iodides that the most accurate and precise experimental data are available.

2. Theoretical Background and Methods

2.1. Mechanisms of the Reduction of In-Crystal Anion Polarizabilities. It is now well established[14,22,23,46] that there are two conceptually different mechanisms which cause anions in-crystal to be more contracted and less polarizable than when isolated. The first of these is that which would arise if all of the surrounding ions were just point charges, whereas the second mechanism is that arising from the overlap between the electron density of an anion with the spatially extended electron densities of the surrounding ions. If the potential acting on an anion electron due to its in-crystal environment is expanded in a multipole series, it is a purely mathematical result[14] that only its spherically symmetric component can affect the electron density of a closed shell ion if it is assumed that this remains spherically symmetric. This is one of the conditions that needs to be fulfilled if a crystal composed of ions of closed shell electron configurations is to be considered fully ionic.[1,14]

For the cubic crystals considered here, the spherically symmetric part of the potential generated by the point charge lattice is a constant attraction from the anion nucleus up to the closest cation−anion separation, beyond which it rises toward zero although there are small oscillations associated with other larger anion−ion separations.[1,46] This potential, illustrated in both Figure 1 of ref 46 and Figure 3 (curve 1) of ref 1, acts as a "confining box"[29] contracting the anion and reducing its polarizability.[22−24,27−30,46]

The second effect on in-crystal polarizabilities arises through the Pauli principle, which effectively introduces an additional repulsion acting on an anion electron in spatial regions in which the electron densities of neighboring ions are not negligible. This repulsion acts to reduce the width of the "confining box" as shown in the lower half of Figure 3 of ref 46 the curve 3 in Figure 3 of ref 1 and as the solid curve in Figure 1 of ref 29 thus augmenting the contractions (see also Figure 1 of ref 29) and polarizability reductions induced by the corresponding point charge lattice.[22−24,27−30,46]

2.2. Procedures for ab Initio Computation of Polarizabilities. The polarizabilities of anions in-crystal can be computed ab initio by considering a single anion embedded in a finite sized portion of the crystal lattice with all other ions except for the closest cation neighbors being treated as point charges.[22−24,30] The outermost charges are adjusted so as to both preserve electrical neutrality of the entire cluster as well as to reproduce the spherical average of the potential experienced by an anion electron.[30] Although this procedure[30] is theoretically preferable to the original approach[22−24] in which the charges were scaled only for the preservation of electrical neutrality, in practice the results of the two methods are virtually identical.[30] In these ab initio computations, it is not necessary either to assume that the ions remain spherically symmetric or to have any prior knowledge of the potential acting on an anion electron. The wavefunctions resulting from the computations will contain both of these types of information, although the analysis needed to derive it has not yet been performed.

Computations, denoted CRYST,[23] in which all of the neighboring ions, including the closest cation neighbors, are treated as point charges yield directly an anion polarizability. Comparison of the results of such computations with those of the corresponding free anion reveals the first of the two in-crystal polarizability modifications, namely those arising from the purely point charge electrostatic effects of the surrounding lattice.[22−24,27−30]

The computation of the polarizability of an anion, taking account of both of the effects contributing to its reduction, requires that the closest cation neighbors are introduced with all their electrons as well as the full nuclear charges. However, a computation, denoted CLUS,[22,23] involving the ab initio treatment of both one anion and plus all its (n_{CA}) closest cation neighbors, with the remaining lattice being represented by point charges, yields the polarizability α_{CLUS} of this entire cluster of anion plus n_{CA} cations. This cluster polarizability contains, in addition to the desired anion polarizability α_A, the cation

polarizability (α_C), the contribution (α_{DID}) from dipole−induced dipole interactions, plus any basis set superposition corrections (α_{BSSE}) which may contribute to α_{CLUS} because the basis sets of either the anion or cations are incomplete.[22] Incompleteness of the basis of any ion can cause its polarizability in the cluster to contain contributions from the basis functions located on neighboring ions. Thus α_{CLUS} is given by

$$\alpha_{CLUS} = \alpha_A + n_{CA}\alpha_C + \alpha_{DID} + \alpha_{BSSE} \qquad (2.1)$$

A basis set for the anion, which is sufficiently large and close to completeness that α_A in CLUS computations does not contain any contributions from cation basis functions, can be constructed by systematically extending the basis until the predicted polarizability is converged. Thus, basis set superposition problems concern only the possible "borrowing" of anion basis functions by cations, thereby modifying the cation polarizability from the known value generated in a computation considering just a single free cation. For lithium salts, these difficulties were elegantly circumvented[22] by using a special [1s1p] basis set in which the 1s function is the Hartree−Fock orbital of a free lithium cation and the 1p function is that ensuring that the Li^+ polarizability is exactly reproduced. The anion polarizability is then extracted from the computed α_{CLUS} by using (2.1) with α_C set to its computed free ion value, α_{BSSE} set to zero with α_{DID} given by[47]

$$\alpha_{DID} = 2n_{CA}(\alpha_A)^2\alpha_C R^{-6} \qquad (2.2)$$

where R is the closest cation−anion separation. This approach is not readily possible for sodium salts because, in the presence of an external perturbing electric field, components of both s and d symmetry are mixed into the wavefunctions for the 2p electrons which are those responsible for the majority of the polarizability. For these salts, a [2s1p] basis set consisting of just the Hartree−Fock orbitals of the free ion was used thus making α_C zero.[23] The resulting nonzero α_{BSSE} could then be computed in a counter-poise computation of the polarizability of the first shell of cations each described by the contracted [2s1p] basis but including also the anion basis functions while excluding the anion electrons and nuclear charge.[23,30] Such a computation including all of the anion basis functions yields an upper bound to α_{BSSE}, whereas, for NaF and NaCl, a similar calculation containing only anion basis functions of d symmetry generates a lower bound.[30] However, the full Na^+ polarizability of some 1 a.u.[23] is sufficiently small that the two counter poise corrections only differ by 0.3 a.u.[30] Since even the smallest anion polarizability, that of the fluoride ion in LiF, is some 6 a.u.,[22] no problems arise from this 0.3 a.u. ambiguity. However, the K^+ polarizability of some 5.4 a.u.[23] is sufficiently large that ambiguities of some 3−4 a.u. enter such a computation of the polarizability of the chloride ion in KCl.[30] This difficulty was circumvented in the present work by computing, for each R, the polarizability of one cation including both its basis functions as well as those anion basis functions, the most diffuse functions, which do not contribute significantly to the anion orbitals occupied in the full CLUS computation. This procedure generates the cation polarizability predicted in-crystal using that basis set, thereby incorporating basis set superposition effects into the value of α_C used in (2.1). This relation with α_{BSSE} set to zero can then be used in conjunction with (2.2) to derive α_A from the computed α_{CLUS}. For Na^+, the [2s1p] Hartree−Fock basis was chosen, whereas the K^+ basis was a [3s2p1d] contraction consisting of the Hartree−Fock orbitals computed for the free ion with the d contraction being that needed to generate all of the contributions to the polarizability that arise from the mixing, in an external electric field, of d symmetry functions into the occupied orbitals. Further details of the extended (21s16p10d4f) → [10s7p5d4f] iodide basis set, the cation sets, and the basis superposition corrections are presented in Appendix 1.

The polarizability of the fluoride ion in LiF deduced from a CLUS computation hardly differs from that predicted in a computation differing only in the removal of all of the point charges,[23] thus leaving only the nuclei and electrons of the closest n_{CA} cation neighbors. This is very strong evidence that both the electrostatic and overlap compression effects from the closest anion neighbors are sufficiently small that they do not require consideration in computations of in-crystal anion polarizabilities.

The polarizabilities at both the Hartree−Fock level and with electron correlation treated by second-order Moller−Plesset perturbation (MP2) theory were derived by comparing the energies computed both with and without the presence in the Hamiltonian of the terms describing the interaction between the electrons and a uniform external electric field. The Hartree−Fock results are thus entirely equivalent to those generated by coupled Hartree−Fock (CHF) computations, whereas the MP2 theory is implemented in its MPE form.[22,23] Although correlation effects in free anions are sufficiently large that the MP2 predictions are not totally reliable, in-crystal the correlation contributions are so reduced as a fraction of the Hartree−Fock terms that the correlation treatment can be restricted to the MP2 approach.[22,23] All of the computations in the present work were performed using the QCHEM quantum chemistry package[48] with Gaussian basis sets.

The reliability of the present computations is not compromised through the neglect of relativistic effects despite the appreciable iodide nuclear charge. Thus, the nonrelativistic CHF prediction of 27.06 a.u[49] for the polarizability of a free xenon atom hardly differs from the relativistic prediction of 26.97 a.u.[50] Although the minimal relativistic contribution might at first seem surprising, it is small because the outermost electrons, namely the 5p, make the dominant contribution to the polarizability. Thus, the eight outermost electrons in Rb^+ contribute 99.5% of the polarizability,[26] whereas the 10 4d electrons in Ag^+ contribute 92%.[25] Valence electron behavior is modified by relativity through two effects, the direct and the indirect.[51] The former, present even in one-electron ions, arises because the valence electron dynamics itself is intrinsically relativistic in that the valence electron orbital is an eigenfunction of a Hamiltonian containing the relativistic Dirac kinetic energy operator rather than the nonrelativistic one. This effect acts to increase the binding energy, contract the orbital, and reduce the polarizability. It is largest for s electrons and decreases with increasing electron angular momentum. The indirect effect arises because the valence electrons in a relativistic treatment are more effectively screened from the nuclear charge as a result of the contractions of the inner orbitals caused by these latter experiencing the direct effect. Consequently, the indirect effect tends to reduce valence orbital binding energies, expand the orbitals, and increase the polarizability. This effect is very small for valence s orbitals and increases with increasing orbital angular momentum. The magnitudes of the direct and indirect effects are almost the same for valence p orbitals thus causing their behavior to be almost unaffected by relativity by virtue of the near cancellation of these two relativistic effects.[51] This cancellation coupled with the dominance of the valence electron contributions to the polarizability explains why the polarizabili-

TABLE 1: Predicted and Experimental Halide Polarizabilities (α_A) in Sixfold-Coordinated (B1) Salts[a]

	LiF	NaF	LiCl	NaCl	LiBr	NaBr	NaI	KI
R_e[b]	3.7965	4.3785	4.8566	5.239	5.197	5.643	6.117	6.676
comp α_A	6.126	7.560	19.563	20.617	27.331	28.839	41.82	43.66
expt α_A	5.983	6.948	19.412	21.153	26.936	28.826	41.85	44.87

[a] All quantities in a.u. Computed α_A all taken from [30] see text, except for iodides, this work. Experimental α_A derived by subtracting the cation polarizabilities computed in ref 23 as presented in ref 25 from experimental molar polarizabilities (α_m) of ref 52. [b] All R_e taken from [29,30] except for NaI and KI from [52].

TABLE 2: Anion Hartree−Fock and Correlation Polarizabilities in B1 Structured Salts at Equilibrium[a]

	F	Cl	Br	I
Li	5.385(0.741, 12%)	18.898(0.665, 3.4%)	26.477(0.854, 3.1%)	
Na	6.378(1.182, 16%)	19.781(0.836, 4.1%)	27.828(1.011, 3.5%)	40.92(0.90, 2.2%)
K				41.75(1.91, 4.4%)

[a] All polarizabilities in a.u. CHF polarizabilities with correlation contributions following in brackets followed by the latter as percentage of the total. Results from ref 30 excepting the iodides, present work.

ties of species belonging to the xenon isoelectronic sequence and of low net charge are hardly affected by relativity.

3. Ab Initio Polarizability Predictions

3.1. Theory and Experiment at Equilibrium Geometries in the B1 Structure. The polarizabilities predicted for halide ions in crystals having the rock-salt (B1) structure at their equilibrium geometries are compared with experimental results in Table 1. All of these predictions include the correlation contributions evaluated using the MPE method. For the fluorides and chlorides, the experimental equilibrium (R_e) closest cation−anion separations reported in the first line of this table were taken from the experiments cited in ref 23, whereas those for the bromides and iodides are from refs 52 and 53, respectively. The polarizabilities predicted for the fluorides, chlorides, and bromides, presented for comparison with present computations for the iodides, are all taken from ref 30. The computations from this source as well the present iodide results are fully comparable because the outermost charges in the point lattice were all constructed using the same prescription. However, it should be pointed out that these anion polarizabilities have been investigated earlier, the results of 6.201 a.u. for LiF, 7.572 a.u. for NaF, 19.376 a.u. for LiCl, 20.932 a.u. for NaCl (all from ref 23), and 28.59 a.u. for NaBr[27] being derived as the sum of the CHF and the average of the MPD and MPE correlation predictions. The very small differences between these, the first predictions,[23,27] and the later results[30] presented in Table 1 arise from the small technical differences in the construction of the outermost point charges as discussed in the appendix of the later paper.

The anion polarizabilities, labeled as experimental in Table 1, were obtained by subtracting from the molar polarizabilities derived from experimental refractive index data extrapolated to infinite wavelength,[52] the reliable values computed[23] for the cation polarizabilities. For NaI and KI, these molar polarizabilities are 42.852 and 50.208 a.u., with Na^+ and K^+ values of 1.002 and 5.339 a.u. The values computed for the polarizability of the iodide ion in both NaI and KI show the same excellent agreement with the experimentally derived values as found previously for the fluorides, chlorides, and bromides. This shows that there is no evidence that this property is significantly affected by any possible slight covalency in these two iodides.

The computed polarizabilities presented in Table 1 are decomposed in Table 2 into their CHF and correlation contributions. Each correlation contribution is also expressed as a percentage of the total prediction presented in Table 1. The result for NaI continues the trend that the fraction of the polarizability arising from electron correlation decreases with increasing anion nuclear charge if the cation is held constant. The results for the iodide ion in both NaI and KI exhibit the same trend shown by the lighter halide ions that the fractional correlation contribution increases with increasing mass of the alkali cation, which, at the equilibrium geometries, means increasing cation−anion separation.

TABLE 3: Free Anion Coupled Hartree−Fock, Second-Order Moller−Plesset and Best Polarizabilities, a.u.[a]

	CHF	MP2	best
F	10.66[49]	16.88 (6.22)[54]	15.1 (4.44)[54,57]
Cl	31.55[49]	37.29 (5.74)[56]	38.01 (6.46)[56]
Br	42.9[27]	46.32 (3.42)[27,30]	
I	60.88	66.00 (5.12)	

[a] CHF and bracketed correlation contributions taken from the indicated references. MP2 totals are the sum of the CHF and bracketed correlation contributions. Correlation contributions to the best results are the best totals minus the CHF values.

3.2. Comparison of Free Anions and Ions in B1 Crystals at Equilibrium. The CHF, MPE, and best current predictions for the polarizabilities of the isolated halide ions are presented in Table 3. For F^-, the CHF values of 10.691[54] and 10.654 a.u.[23] derived from conventional quantum chemistry computations using basis sets are all essentially identical with the Table 3 result of the numerical computations.[49] The basis set predictions of 31.56,[55] 31.49,[56] and 31.468 a.u.[23] for Cl^- are also essentially identical to the numerical CHF result[49] presented in Table 3. The most accurate Br^- CHF prediction of 42.9 a.u. derived from the larger of the two basis sets[27] is greater than that of 38.3 a.u. computed from the smaller basis. The most reliable MPE values for the correlation polarizability, presented in brackets in the second numerical column of Table 3, yield, after addition of the CHF values, the total polarizability predicted by MPE theory. For the F^- ion, the MPE correlation polarizability of 6.090 a.u.[23] is very similar to the 6.22 a.u. value[54] presented in Table 3. Furthermore, the predictions of 5.61[23] and 5.69 a.u.[55] for the MPE correlation polarizability of the Cl^- ion are very similar to the best current value of 5.74 a.u.[56] reported in Table 3. The only value for the correlation polarizability of a free Br^- ion (Table 3) is the MPE result computed[27,30] using the smaller of the two basis sets considered in ref 27. The previously reported[29,30] value of 41.72 a.u. for the total polarizability derived by adding to 3.42 the 38.3 a.u. CHF prediction[27,30] of the same smaller basis set is therefore less

TABLE 4: Computed Anion Polarizabilities Including Correlation, Correlation Contributions Bracketed[a]

	NaI			KI		
	4:4	6:6	8:8	4:4	6:6	8:8
2.1	31.88(0.72)	25.83(0.10)				
2.4	33.76(0.57)	28.11(-0.09)			29.00(1.83)	
2.7	37.73(0.68)	32.97(0.48)			31.59(1.44)	
3.0	41.98(0.98)	37.78(0.58)	37.41(0.45)	39.18(1.46)	35.13(1.46)	32.84(1.48)
3.2	45.06(1.27)		38.60(0.69)	42.63(1.93)		35.83(1.59)
3.3		42.86(1.03)			39.94(1.79)	
3.4	48.82(1.82)		41.84(1.03)	44.81(2.11)		39.00(1.74)
3.5		46.36(1.44)				
3.6	51.90(2.28)		45.72(1.43)	48.13(2.37)		42.61(1.95)
3.8	55.03(2.56)	51.32(2.05)	49.37(1.86)	51.36(2.65)	48.59(2.25)	46.18(2.20)
4.0	57.30(2.93)		52.65(2.02)	54.16(2.98)		50.16(2.62)
4.2	59.60(3.35)	56.55(2.93)	55.43(2.70)	56.85(3.33)	54.66(3.02)	53.34(3.04)
4.5	62.38(3.98)	59.49(3.46)	58.56(3.24)	59.57(3.37)	58.31(3.56)	57.72(3.64)
4.8	64.39(4.37)	61.53(3.90)	60.18(3.81)	62.54(3.89)	60.96(3.97)	60.34(4.17)

[a] Separations in angstroms and polarizabilities in a.u.

than the more accurate 46.32 a.u. result in Table 3 derived from the 42.9 a.u. CHF value. The most accurate computations of the free F^- polarizability are those yielded from either Moller−Plesset perturbation theory carried through to fourth order (MP4)[57] or from the MC−CCI method.[54] Both approaches predict the same 15.1 a.u. result in Table 3. For the Cl^- ion, the most accurate predictions are those of MP4 theory; the result of 37.5a.u.[55] is very similar to the later MP4 result[56] presented in Table 3. The best value (Table 3) for each of the correlation polarizabilities is the difference between the total and the CHF value presented in that table.

The results in Table 3 show that the CHF contributions to the free anion polarizabilities increase very significantly with increasing nuclear charge. However the data in Table 3 also show that, compared with both this rapid increase and greater magnitudes of the CHF free anion polarizabilities, the correlation polarizabilities are roughly constant. The only available value for the correlation polarizability of Br^-, namely, the MPE result of 3.42 a.u., is almost certainly too small because this was computed using the smaller of the two basis sets which is known to underestimate the CHF contribution. Significantly increasing CHF terms coupled with smaller and roughly constant correlation contributions cause the correlation polarizability to constitute a decreasing fraction of the total polarizability as nuclear charge increases.

The anion correlation polarizabilities in the B1 structured sodium salts at equilibrium are almost constant in both absolute terms at about 1 a.u. (Table 2) and as a fraction of some 20% of the free ion correlation terms (Table 3). Since the fractional reductions in the CHF terms of 50%, 41%, 36%, and 33% on passing from each free ion to that in its sodium salt are much less than a 5-fold reduction of the correlation contributions, these latter constitute a much smaller fraction of the total polarizability in-crystal. As the anion nuclear charge increases, the decrease of the reductions in the CHF polarizabilities coupled with the constant fractional reduction of the correlation terms explains why these latter constitute an increasing yet still very small fraction of the total on descending the group.

3.3. Distance and Structural Dependencies of the Anion Polarizability. The total anion polarizabilities predicted as a function of closest cation−anion separation (R) for three different cubic phases of both NaI and KI are presented in Table 4. The correlation contributions, presented in brackets in the table, were derived from the results of MPE computations. The three polymorphs considered are the 4-fold coordinated phase having the zinc blende (B3) structure, the 6-fold coordinated rock salt (B1) structure adopted by these salts under ambient conditions, and the 8-fold coordinated phase having the cesium chloride (B2) structure observed at high pressures.

The results show, as should be expected from previous work,[28−30] that the anion polarizabilities increase with both decreasing coordination number at constant distance and with increasing distance at constant coordination number. At constant R, the polarizability in the potassium salt is smaller than that in the sodium salt having the same structure. This would be expected because the greater spatial extent of the K^+ electron density will, through the operation of the Pauli principle, exert a greater compressive influence on the anion density. The data show that each of the six polarizabilities exhibits the sigmoid dependence on internuclear distance found previously[29,32] for the salts containing the lighter halogens.

For each structure of each salt at the smallest R, the correlation polarizability (Table 4) decreases with increasing R till it reaches a minimum after which it increases with increasing R to tend toward the free ion value presented in Table 3. The electron density in a more compressed ion is more localized in spatial regions where the attraction to the positively charged core of nucleus plus inner electrons is higher. This greater influence of the attraction to the core will tend to outweigh the repulsions between the outermost electrons thereby decreasing the correlation polarizability. However, in the very compressed anions occurring at very small R, it could be envisaged that the outermost electrons are so close that their augmented repulsions are sufficiently large as to outweigh the effects of their attractions to the core resulting in an increased correlation contribution to the polarizability. The result of a comparison between the correlation polarizabilities of different polymorphs at the same R or between those in the same polymorphs at the same R of different salts will depend on whether R is greater than both of those yielding the minimum correlation contribution in each system. The more compressed ion of smaller total polarizability will only definitely have smaller correlation polarizability for R greater than both these minima. Thus, it is only for the larger R considered in Table 4 that the correlation polarizability in each salt decreases with increasing coordination number at constant R. The seemingly less straightforward results of other comparisons of the correlation polarizabilities can be attributed to differences in the R at which the correlation polarizabilities are minimized.

3.4. Computed and Experimental Molar Polarizability Distance Derivatives. Experimentally based values for the derivative $[d\alpha_A/dR]_{R=R_e}$ of the anion polarizability with respect

TABLE 5: Computed and Experimental Derivatives of Anion Polarizability with Respect to Distance[a]

	LiF	NaF	LiCl	NaCl	LiBr
n_∞	1.3878	1.3210	1.6463	1.5278	1.752
no or $[V\mathrm{d}\epsilon_\infty/\mathrm{d}V]_{V=V_e}$	9	6	(−0.573)[b]	8	(−0.653)[b]
expt $[\mathrm{d}\alpha_A/\mathrm{d}R]_{R=R_e}$	3.407 ± 0.118	3.610 ± 0.690	(9.650)	6.990 ± 0.293	(12.844)
comp $[\mathrm{d}\alpha_A/\mathrm{d}R]_{R=R_e}$	3.22	3.14 − 3.21	6.466	6.05 (6.26)	8.05

	NaBr	NaI	KI	RbI
n_∞	1.6126	1.7305	1.6275	1.650
no or $[V\mathrm{d}\epsilon_\infty/\mathrm{d}V]_{V=V_e}$	3	−1.6959[c]	7	−1.446[c]
expt $[\mathrm{d}\alpha_A/\mathrm{d}R]_{R=R_e}$	9.050 ± 0.601	10.473	10.570 ± 0.754	9.24
comp $[\mathrm{d}\alpha_A/\mathrm{d}R]_{R=R_e}$	6.89 − 6.94	9.573	9.314	

[a] n_∞ from ref 58. No or $[V\mathrm{d}\epsilon_\infty/\mathrm{d}V]_{V=V_e}$: An integer denotes the number of independent experiments (see Appendix 2). $[\mathrm{d}\alpha_A/\mathrm{d}R]_{R=R_e}$ in a.u. Comp $[\mathrm{d}\alpha_A/\mathrm{d}R]_{R=R_e}$: F^-, Cl^-, and Br^- from ref 29. I^- present work. [b] $[V\mathrm{d}\epsilon_\infty/\mathrm{d}V]_{V=V_e}$ from refs 59 and 60 calculated using the method of fractional change. Values bracketed are not truly experimental. [c] $[V\mathrm{d}\epsilon_\infty/\mathrm{d}V]_{V=V_e}$ derived from experimental data (see Appendix 2).

to closest cation−anion separation can be derived[29] by combining knowledge of ϵ_∞, the crystal high-frequency dielectric constant extrapolated to infinite wavelength, with that of its volume dependence as expressed by the dimensionless quantity $[V\mathrm{d}\epsilon_\infty/\mathrm{d}V]_{V=V_e}$. The latter can either be measured directly or readily deduced from a variety of different experiments in each of which standard relations are used to combine two different measured quantities. These relations and the experimental data are presented in Appendix 2. The relationship between $[\mathrm{d}\alpha_A/\mathrm{d}R]_{R=Re}$ and these two experimental quantities is most readily derived by differentiating with respect to the molar volume (V), the expression for α_m, the molar polarizability, provided by the Clausius−Mossotti equation.

$$\alpha_m = [3V/(4\pi)][\epsilon_\infty - 1]/[\epsilon_\infty + 2] \qquad (3.1)$$

After taking the cation polarizability to be a constant independent of V and then expressing $\mathrm{d}\alpha_A/\mathrm{d}V$ in terms of $\mathrm{d}\alpha_A/\mathrm{d}R$, one obtains

$$[\mathrm{d}\alpha_A/\mathrm{d}R]_{R=R_e} = \{9R_e^2/[2\pi(\epsilon_\infty + 2)]\} \{\epsilon_\infty - 1 + [3/(\epsilon_\infty + 2)][V\mathrm{d}\epsilon_\infty/\mathrm{d}V]_{V=V_e}\} \qquad (3.2)$$

where V_e ($=2R_e^3$ for B1 structured alkali halides) is the molar volume at the equilibrium geometry. A relation equivalent to (3.2) appears as eq 16 of ref 28 after noting that the quantity $f\alpha_A(R)$ is just $\mathrm{d}\alpha_A(R)/\mathrm{d}R$. This form can be rearranged to (3.2) by substituting for $\alpha_m(R)$, the expression provided by the Clausius−Mossotti equation. The values of R_e entering (3.2) were taken from Table 1, whereas those of ϵ_∞ were calculated as the square of the most recent experimental values[58] of n_∞ (Table 5), the refractive index extrapolated to infinite wavelength. For five of the salts considered, a number of different experimentally deduced values for $[V\mathrm{d}\epsilon_\infty/\mathrm{d}V]_{V=V_e}$ are available. These are assembled in Appendix 2 together with their derivation from the directly measured primary data, which is also reported. For each of the remaining salts, the only available value for $[V\mathrm{d}\epsilon_\infty/\mathrm{d}V]_{V=V_e}$ is presented with its source in Table 5. The error limits presented in Table 5 for each of the experimentally deduced values of $[\mathrm{d}\alpha_m/\mathrm{d}R]_{R=R_e}$ were calculated by giving equal weight to all the different determinations.

The values of $[\mathrm{d}\alpha_A/\mathrm{d}R]_{R=R_e}$ deduced from (3.2) are compared with the predictions of the MPE ab initio computations in the two lowest lines of Table 5. The MPE results for the fluorides, chlorides, and bromides are taken from the previous work.[29] Those for the iodides were derived by fitting the MPE ab initio results (Table 4) to the "logistic function"

$$\alpha_A = a_0 + a_1[1 + \exp(a_2 - a_3R)]^{-1} \qquad (3.3)$$

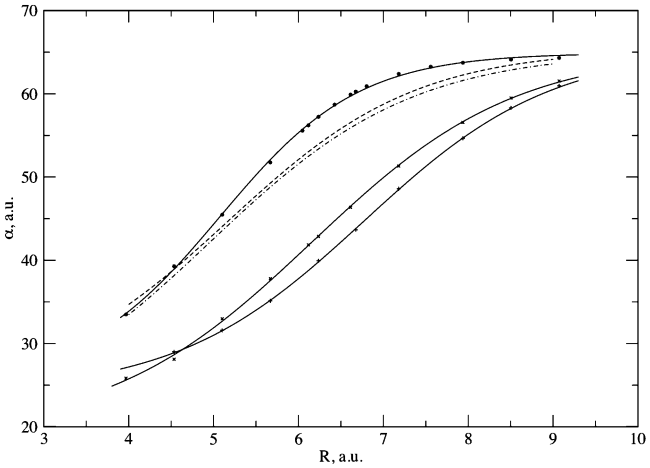

Figure 1. MPE iodide polarizability for the 6-fold coordinated structure of NaI (denoted by ×) and KI (denoted by +) as well as in the point charge lattice (denoted by *) fitted to the logistic function (3.3) (solid line). Dashed sigmoid curves show the distance dependence of the MPE iodide polarizabilities for NaI and KI predicted by the "shifted point lattice model"[29] as described in the text (paragraph 4.1).

TABLE 6: Parameters in (3.3) Describing the MPE $\alpha_A(R)$ in Rock Salt Structured NaI and KI (a.u.)

	a_0	a_1	a_2	a_3
NaI	19.273	45.84	5.147	0.8356
KI	24.059	41.35	6.116	0.9028
point lattice	25.543	39.36	6.215	1.2249

with the values of the coefficients being presented in Table 6. The solid curves in Figure 1 confirm the goodness of these fits. The quality of the agreement between the ab initio predictions and those derived from (3.2) might appear to be somewhat variable. However, it should be pointed out that the greatest discrepancies arise for those systems, namely LiCl and LiBr, for which the results derived from (3.2) relied on values of $[V\mathrm{d}\epsilon_\infty/\mathrm{d}V]_{V=V_e}$ which do not originate from experiment. For these two systems, the $[V\mathrm{d}\epsilon_\infty/\mathrm{d}V]_{V=V_e}$ values in Table 5 were estimated[59] using the method of fractional change.[60] Evidence that this method significantly overestimates $[\mathrm{d}\alpha_A/\mathrm{d}R]_{R=R_e}$ is provided by the case of NaI for which this method yields[59] a value of −1.280 for $[V\mathrm{d}\epsilon_\infty/\mathrm{d}V]_{V=V_e}$ which is significantly different from that of −1.6959 (Table 5) derived directly from experiment. The former value for $[V\mathrm{d}\epsilon_\infty/\mathrm{d}V]_{V=V_e}$ yields a prediction of 13.154a.u for $[\mathrm{d}\alpha_A/\mathrm{d}R]_{R=Re}$ in NaI, which is significantly greater than the experimental value of 10.473 a.u. The ranges of values quoted for the $[\mathrm{d}\alpha_A/\mathrm{d}R]_{R=Re}$ computed for NaF, NaCl, and NaBr arise from the small uncertainties in the derivation of the basis set superposition errors as discussed

elsewhere.[29,30] The bracketed upper limit in Table 5 for the 6.05 a.u. value computed[29] for the NaCl $[d\alpha_A/dR]_{R=R_e}$ is derived by adding 0.21 a.u. The latter quantity is the range of $[d\alpha_A/dR]_{R=R_e}$ arising in the corresponding CHF computations,[29] no range of MPE results being presented.

For two of the six crystals considered in Table 5 for which true experimentally derived values of $[d\alpha_A/dR]_{R=Re}$ are available, namely LiF and NaF, the ab initio predictions would seem to agree closely with the experimental results after noting the estimated errors of the latter for each crystal. However, the ab initio predictions for NaCl, NaI, and KI would seem to underestimate slightly the experimentally derived results. The larger discrepancy between theory and experiment for NaBr might well arise from the slightly nonoptimal nature of the smaller Br basis which, for the free ion, underestimates the CHF polarizability while also probably yielding too smaller correlation polarizability as discussed in section 3.2. However, the results for the six systems for which true experimental values of $[Vd\epsilon_\infty/dV]_{V=V_e}$ and hence $[d\alpha_A/dR]_{R=R_e}$ are available, do not constitute body of evidence sufficiently large for it to be known whether partial covalency or some other effect is responsible for the agreement between theory and experiment being less satisfactory than for the polarizabilities themselves. It is also beyond the scope of this paper to reinvestigate the basis sets used for the chlorides, bromides, and iodides.

4. Physical Models for the Environmental Dependency of Anion Polarizabilities

4.1. Model for Cation Dependence of Anion Polarizabilities in the B1 Phases. A variety of models for the environmental dependence of anion polarizabilities have been developed[25,29,32,33,52] with the twin objectives of providing a conceptual framework for understanding such variations on a unified basis and of deriving numerical values for systems too large or inconvenient for ab initio computation. Each of these models has proved useful in unifying different classes of data. The model of Wilson and Curtis,[52] when regarded as an empirical fitting scheme, has proved to be invaluable[25] in relating the polarizabilities of the same anion in different crystals all at their equilibrium geometries even if the questionable physical basis of this model is not accepted. The object here is to discuss and test the applicability to iodides of the model,[29] to be called the "shifted point lattice model", which places on a unified basis encompassing both all counter cations and all internuclear distances, the polarizabilities of each anion in a B1 structured crystal.

The basic idea of the "shifted point lattice model"[29] is that the sigmoid-shaped dependence on R of α_A in a crystal can be generated by shifting along the R axis the sigmoid-shaped curve describing the polarizability of the same anion in the point charge lattice having the same structure. This idea gains physical content beyond the observation that the curves can be thus superimposed by the further result that the shift is a constant for any cation, being therefore independent of the anion.[29] Thus, denoting the polarizability of anion A in its salt with cation C with closest cation−anion separation R by $\alpha_A^{CA}(R)$, with $\alpha_A^{PL}(R)$ the polarizability in the corresponding point lattice, the model states that

$$\alpha_A^{CA}(R) = \alpha_A^{PL}(R - \delta_C) \qquad (4.1)$$

where δ_C is defined solely by the cation. For fluorides and chlorides, it was shown[29] for the MP2 predictions of $\alpha_A^{CA}(R)$ in B1 structured salts that δ_{Li^+} and δ_{Na^+} took the respective values of 0.9 and 1.2 a.u. A further scaling in which both sides of (4.1) are divided by the free anion polarizability allowed the CHF predictions of to be scaled onto those of the MP2 computations by a constant anion-independent shift.[29] This will not be further considered since the MP2 polarizabilities, which have been shown to yield results close to experiment, satisfy (4.1) without any further scaling.

TABLE 7: Internuclear Separations R_e and Polarizabilities α_A in B1 Structures from Experiment[a]

	KF	RbF	KCl	RbCl	CsF	CsCl	RbI
R_e	4.517	4.765	5.316	5.561	5.081	6.689	6.935
expt α_A	8.104	8.374	22.856	23.410	9.176	24.319	45.81

[a] All quantities in a.u. All R_e from ref 52 except for CsCl from ref 53. All experimental α_A (denoted $\alpha_A^{CA}(R_e)$ in section 4.1), excepting CsCl, derived by subtracting the cation polarizabilities[23,25] from experimental molar polarizabilities (α_m) of ref 52 CsCl α_A is taken from ref 17.

The view that the MP2 and exact polarizabilities are essentially interchangeable allows the in-crystal MP2 polarizability appearing on the left of (4.1) to be replaced by the experimental polarizability for $R = R_e$. It is then possible to deduce values of δ_C for heavier cations for which a CLUS type ab initio computation of anion plus six such cations is not readily feasible either due to computational limitations or basis superposition problems. These δ_C's are determined through (4.1) by equating to $R_e - \delta_C$ the distance R at which the anion polarizability $\alpha_A^{PL}(R)$ in the point lattice equals the experimental in-crystal value $\alpha_A^{CA}(R_e)$. For the fluoride and chloride ions, the required functions $\alpha_A^{PL}(R)$ of R are depicted in Figure 2, panels a and b, of ref 29. Each of the required values of $\alpha_A^{CA}(R_e)$ presented in Table 7, excepting that for CsCl, was derived by subtracting the cation polarizability from the experimental molar polarizability α_m. Although the B1 phase of CsCl is observed at high temperatures thus providing an experimental distance R_e, a value of α_m and hence $\alpha_A^{CA}(R_e)$ is not available from experiment. However, it has been shown[17] that the latter can be reliably predicted from the known R_e by using the relation (1) of ref 25 with coefficients taken from Table 3 of that paper. Application of (4.1) to the data for RbF and RbCl yields values of 1.8 and 1.7 a.u., respectively, for δ_{Rb^+}, suggesting a final average value of 1.75 a.u. Values of 1.91 and 1.98 a.u. are similarly derived from the data for CsF and CsCl thereby yielding a value of 1.95 a.u for δ_{Cs^+}. Although the δ_{Cs^+} value falls within the range that might be expected, that for δ_{Rb^+} seems surprisingly close to that of 1.7 a.u. reported for δ_{K^+}.[29] However, the latter was derived using the MPE prediction of 6.7045 a.u. for α_F in KF which is significantly less than the experimental value (Table 7) of 8.104 a.u. Use of the experimental anion polarizabilities in KF and KCl yields respective values of 1.63 and 1.57 a.u. for δ_{K^+}. The resulting average value of 1.60 a.u. would appear to be more in line with those of 1.2 and 1.75 a.u. for δ_{Na^+} and δ_{Rb^+} . A complementary graphical representation of these procedures is depicted in Figure 1 of ref 32.

For the iodide ion, the distance dependence ($\alpha_A^{PL}(R)$ presented in Table 8) of its polarizability in a point lattice was computed by both the CHF and MPE methods with the same basis set used for the both the free ion and CLUS calculations. In the absence of any ab initio computations, the previous treatment[32] of iodides had to invoke two assumptions. The first was that the function $\alpha_A^{PL}(R)/\alpha_A^{PL}(R = \infty)$ for the iodide ion is the same as that for Br^- and second that the polarizability of the free iodide ion $[\alpha_A^{PL}(R = \infty)]$ could be estimated by extrapolating data for the lighter halogens. The present MPE

TABLE 8: MPE Polarizabilities of Iodide in B1 Structured Point Charged Lattices[a]

R	$\alpha_A^{PL}(R)$	R	$\alpha_A^{PL}(R)$	R	$\alpha_A^{PL}(R)$	R	$\alpha_A^{PL}(R)$
2.1	33.50(-0.40)	2.4	39.28(0.24)	2.7	45.48(0.86)	3.0	51.75(1.79)
3.2	55.57(2.48)	3.237	56.21(2.60)	3.3	57.23(2.81)	3.4	58.69(3.12)
3.5	59.90(3.40)	3.5328	60.26(3.48)	3.6	60.91(3.63)	3.8	62.39(4.01)
4.0	63.25(4.25)	4.2	63.73(4.40)	4.5	64.12(4.54)	4.8	64.31(4.61)

[a] Separations R in angstroms, and polarizabilities $\alpha_A^{PL}(R)$ in a.u., with correlation contributions in brackets.

TABLE 9: Experimental and "Shifted Point Lattice" Predictions for α_A and $[d\alpha_A/dR]_{R=R_e}$ (a.u.)[a]

	$\alpha_A^{CA}(R_e) = \alpha_A$			$[d\alpha_A/dR]_{R=R_e}$		
	NaI	KI	RbI	NaI	KI	RbI
model	43.33	43.75	46.56	11.94	12.05	12.60
expt	41.85	44.87	45.81	10.47	10.57	9.24

[a] Model predictions computed from eq 4.1 as described in the text. For sources of experimental results, see footnote a in Table 1 and Appendix 2.

prediction of 66.0 a.u. for the latter shows that the estimate[32] of 58.0 a.u. is slightly too small, while furthermore each halide ion has its own unique $\alpha_A^{PL}(R)/\alpha_A^{PL}(R = \infty)$ curve. The MPE predictions for $\alpha_A^{PL}(R)$ with their correlation contributions bracketed are presented in Table 8 and depicted as the upper curve in Figure 1. The results show the now well established and understood trends of the polarizabilities being smaller than that of the free ion but larger than those predicted by the CLUS computations for the actual NaI and KI crystals. Furthermore, although the correlation contributions in the point lattice are suppressed relative to that in the free ion, this contribution at each distance R is larger both in absolute terms and as a percentage than that in the NaI and KI CLUS computations. Thus, in the point lattice, both the total polarizability and its correlation contribution are suppressed relative to those in the free ion but to a lesser degree than in the presence of the cations with their attendant electrons.

The R dependence of $\alpha_A^{PL}(R)$ was fitted to (3.3) with the values of the parameters being reported in the last line of Table 6. It can be seen from Figure 1 that the distance dependence of $\alpha_A^{CA}(R)$ for neither NaI nor KI can be reproduced by shifting the point lattice function $\alpha_A^{PL}(R)$. Although $\alpha_A^{CA}(R)$ for KI might, disregarding the difference in shape, be roughly regarded as being shifted from $\alpha_A^{PL}(R)$ by the 1.60 a.u. value for δ_{K^+} derived from the data for KF and KCl, the $\alpha_A^{CA}(R)$ curve for NaI is certainly displaced by more than the 1.2 a.u. value for δ_{Na^+} established from the data for NaF, NaCl, and NaBr. In contrast to the fluorides, chlorides and bromides previously examined,[29] the iodide $\alpha_A^{PL}(R)$ increases significantly more rapidly toward the free ion polarizability than does $\alpha_A^{CA}(R)$ in either NaI or KI. The values for both the iodide polarizability and its distance derivative derived by replacing R_e by $R_e - d_C$ in (4.1) are presented in Table 9. Although the model predicts each individual iodide polarizability to an accuracy of about 3%, it fails to provide a satisfactory description of their differences. Furthermore, not only does the model overestimate $[d\alpha_A/dR]_{R=R_e}$ but also it erroneously predicts that this quantity is larger for RbI than for KI. The origin of these difficulties of the model is revealed by Figure 1 because this shows that the point lattices $[d\alpha_A/dR]_{R=R_e}$ are significantly greater than those in the actual salts.

4.2. Model for the Distance and Structural Dependencies of Anion Polarizabilities. A model, called the light scattering model,[33] was developed to describe the dependence of the polarizability of a given anion on the positions of other ions.

TABLE 10: Parameters Describing the MPE $\alpha_A(R)$ in the Light Scattering Model (a.u.)

	a_0	a_{CA}	c_{CA}	a_{AA}	c_{AA}
NaI, eq 4.3	0.0148	0.059	0.605		
NaI, eq 4.4	0.0147	0.0761	0.632	−0.520	1.0984
KI, eq 4.3	0.0148	0.090	0.635		
KI, eq 4.4	0.0144	0.1775	0.638	−0.309	0.7623

The objective of this model was to describe all such environments that could be generated by a given set of ions thereby enabling the model to be introduced into molecular dynamics simulations used to investigate the behavior of ions in melts and disordered systems. In this approach, based on the Drude model for polarizability, the polarizability of an ion X of unit charge is given by

$$\alpha_X = 1/\{a_0 + \sum_Y a_{XY} \exp(-c_{XY} r_{XY})\} \qquad (4.2)$$

where the sum over Y is over all ions other than X, with ion Y being located at a distance r_{XY} from ion X. The constants a_0, a_{XY}, and c_{XY} are determined by fitting (4.2) to the polarizabilities in a known environment that have already been independently determined. One clear physical implication of (4.2) is that $1/a_0$ should equal the polarizability of the free ion X.

For the cubic crystals considered in this paper, (4.2) reduces to the form

$$\alpha_A(R) = 1/\{a_0 + n_{CA} a_{CA} \exp(-c_{CA} R)\} \qquad (4.3)$$

if only the n_{CA} closest cation neighbors are taken to influence the anion polarizability. This view is first supported by the previous result[23] that the polarizability of the fluoride ion in LiF deduced from a CLUS computation hardly differs from that predicted in a calculation differing only in the removal of all of the point charges. Second, it is reinforced by the present result that the 42.55 a.u. value, predicted for the iodide polarizability in NaI at its equilibrium geometry in a CLUS calculation with all the point charges removed, is very similar to that of 41.82 a.u. yielded from the full CLUS computation (Table 1). The parameters resulting from fitting (4.3) to the data of Table 4 for B1 structured NaI and KI are presented in Table 10. Inspection of Figures 2 and 3 shows that the function (4.3) does not provide a very good description of $\alpha_A(R)$ in either salt with the worst discrepancies arising at small R. These figures also depict the anion polarizabilities predicted from (4.3) for the 4 and 8-fold coordinated phases using the basic idea of the light scattering model that a_0, a_{CA}, and c_{CA} are constants with only the coordination number n_{CA} being changed. It is seen, as found previously[29] for the lighter halides, that the formula (4.3) overestimates the anion polarizabilities in the 4:4 phase while underestimating them in the 8:8 materials.

It is possible to consider also the effects of the closest anion neighbors when applying (4.2) to the cubic crystals when this becomes

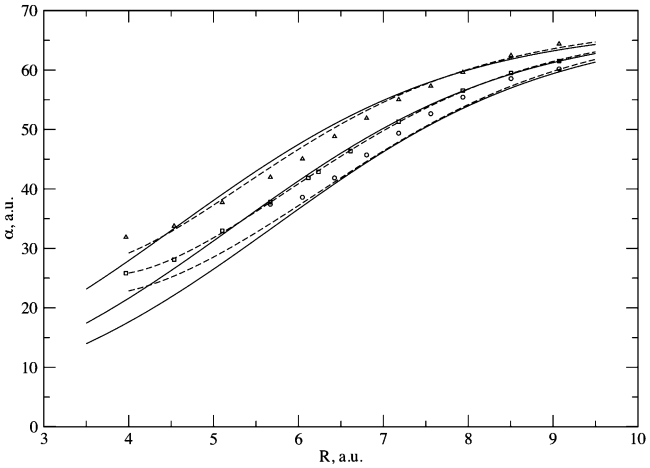

Figure 2. MPE iodide polarizability for the 4-fold (denoted by triangles), the 6-fold (denoted by squares), and the 8-fold coordinated structure (denoted by circles) of NaI fitted using the light scattering model.[33] Solid lines correspond to the fitting with the use of formula (4.3), and dashed lines correspond to the fitting with the use of formula (4.4).

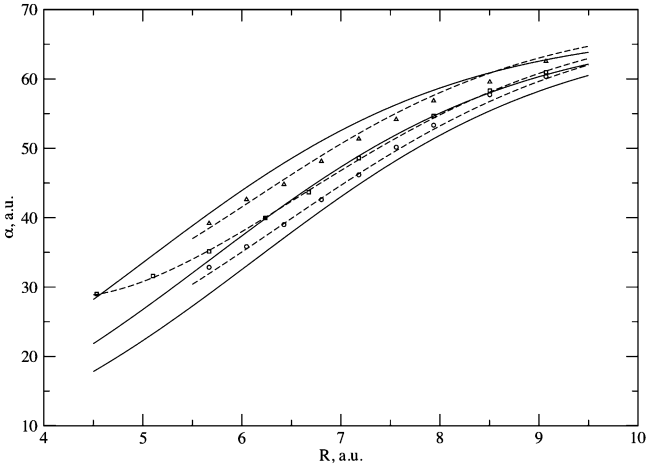

Figure 3. MPE iodide polarizability for the 4-fold (denoted by triangles), the 6-fold (denoted by squares), and the 8-fold coordinated structure (denoted by circles) of KI fitted using the light scattering model.[33] Solid lines correspond to the fitting with the use of formula (4.3), and dashed lines correspond to the fitting with the use of formula (4.4).

$$\alpha_A(R) = 1/\{a_0 + n_{CA}a_{CA}\exp(-c_{CA}R) + n_{AA}a_{AA}\exp(-c_{AA}x_{AA}R)\} \quad (4.4)$$

Here x_{AA} is a purely geometrical constant which yields the separation between anion A and any of its n_{AA} closest anion neighbors as $x_{AA}R$. The quantities a_{AA} and c_{AA} are two further parameters to be determined by fitting (4.4) to known polarizability data. For both NaI and KI, all five of the a and c parameters, presented in Table 10, were again fitted to reproduce the anion polarizabilities in the 6-fold coordinated salts. However, parameters resulting from this procedure cannot in general be given the interpretation implied by the physics of the original model, namely that the denominators in (4.3) and (4.4) are force constants acting on anion electrons in a Drude type model with the terms $n_{CA}a_{CA}\exp(-c_{CA}R)$ and $n_{AA}a_{AA}\exp(-c_{AA}x_{AA}R)$ representing the separate contributions from respectively the closest cation and anion neighbors. Thus, for the salts examined in Table 4 of ref 29 the values of $\alpha_A(R)$ that result from the parameters in that Table by including only a_0 and the cation−anion term in (4.4) are significantly too large. Reasonable results are only obtained by including also the anion−anion contributions. This shows that parameter sets, such those in Table 10, are in general unphysical because the ab initio results show that introduction of the rest of the lattice beyond the closest cation neighbors hardly changes the predicted anion polarizability. Thus, in contrast to (4.4) with both the parameters in Table 4 of ref 29 and the KI parameters of Table 10, the majority of the in-crystal suppression of the anion polarizability is induced solely by the closest cation neighbors. For example, use of (4.4) without including the anion−anion term coupled with the parameters in Table 4 of ref 29 predicts the anion polarizability in LiF to be 8.92 a.u. which is significantly larger than either the experimental value or the ab initio result predicted by including only the six closest cation neighbors. Furthermore, the anion polarizability in KI is predicted to be only 33.95 a.u. if the anion−anion term in (4.4) is not included, a satisfactory prediction of 43.82 au. only arising on introducing this term. It is only for NaI that the Table 10 parameters are not unreasonable. For this salt, the anion−anion terms play a minor role, the prediction of 41.22 a.u. derived from (4.4) excluding the anion−anion term differs only slightly from that of 43.82 a.u. predicted from the full formula.

The observations in the previous paragraph do not imply any criticism of the light scattering model, only that determination of the parameters in (4.4) by fitting to the just the total polarizabilities in Table 4 is questionable. The physically soundly based procedure is first to perform a series of ab initio computations of $\alpha_A(R)$ in which the anion is surrounded by just the six closest cation neighbors and to fit the results to (4.3). Then the ab initio results (Table 4) for the polarizabilities in the full lattice should be fitted to (4.4) but keeping the values of a_0, a_{CA}, and c_{CA} unchanged from the previous first fit. This would ensure that the resulting anion−anion parameters a_{AA} and c_{AA} were sufficiently small that this term really does describe the much smaller influence of the ions beyond the closest cation neighbors. The performance of such a series of ab initio computations, however, lies beyond the scope of the present paper.

It is seen from Figure 2 that the anion polarizabilities in the 4 and 8-fold coordinated NaI predicted from (4.4) are hardly changed from the mediocre predictions afforded by (4.3). Thus, iodide exhibits a different behavior from the fluorides previously examined[29] for which this procedure faithfully reproduces the ab initio polarizabilities. However, Figure 3 shows that the anion polarizability in KI behaves similarly to the fluorides[29] in that the relation (4.4) does reasonably reproduce the values in both the 4:4 and 8:8 phases.

5. Conclusions

The polarizability of the iodide ion in three different cubic polymorphs of solid NaI and KI, the 4-fold coordinated zinc blende structure, the 6-fold coordinated rock salt structure, and the 8-fold coordinated phase having the CsCl structure has been derived as a function of the cation−anion separation (R) from ab initio electronic structure computations. The contributions from electron correlation were computed using Moller-Plessett perturbation theory taken to second order. For both NaI and KI, the anion polarizability predicted for the observed rock-salt polymorph at the equilibrium separation agrees well with the value deduced from experiment by subtracting the known cation polarizability from the experimental molar polarizability deduced through the Clausius−Mossotti equation from refractive index measurements. The computed results show, as expected, that the anion polarizabilities increase with both decreasing

coordination number at constant distance and with increasing distance at constant coordination number. At constant *R*, the polarizability in the potassium salt is smaller than that in the sodium salt having the same structure. For each of the three polymorphs of both NaI and KI, the correlation contribution to the polarizability decreases with increasing *R* at small *R* till it reaches a minimum after which it increases with increasing *R* to tend toward the free ion value.

For the rock-salt phases of both NaI and KI, the polarizability derivative $[d\alpha_m/dR]_{R=R_e}$ was calculated from the function (3.3) describing the distance dependence of the anion polarizability. The predicted values are slightly less than those deduced from the experiment although the percent underestimations in the region of some 10% are no greater than those found previously[29] for those fluorides, chlorides, and bromides for which reliable experimentally derived data is available.

The distance dependence $\alpha_A^{PL}(R)$ of the anion polarizability in the representation of the rock-salt lattice in which all ions other than one anion are replaced by point charges was computed as the key function in the previously introduced[29] "shifted point lattice model". This model states, as shown by eq 4.1, that the function describing the distance dependence of the anion polarizability in any salt is given by shifting the point lattice function $\alpha_A^{PL}(R)$ along the *R* axis by a constant depending only on the cation. Values for the shifts appropriate to K^+, Rb^+, and Cs^+ were derived from the $\alpha_A^{PL}(R)$ previously computed for the F^- and Cl^- ions[29] and found to be anion independent as predicted. For the iodide ion, the distance dependence of $\alpha_A^{PL}(R)$ is well described by the functional form (3.3). However, the function $\alpha_A^{PL}(R)$ is slightly but significantly different in shape, rising more rapidly toward the free ion value, than either of the functions $\alpha_A(R)$ for NaI and KI. This difference causes the values predicted from the (4.1) for the polarizability derivatives $[d\alpha_m/dR]_{R=R_e}$ in NaI and KI to be significantly greater than either the ab initio or experimentally derived results. Even the predictions for the polarizabilities themselves, although not unsatisfactory, fail to describe the observed in-crystal cation dependencies. Thus, these results are not of the same high quality as those previously found[29] for the lighter halides. For salts of each of these latter three halides, the in-crystal polarizability functions $\alpha_A(R)$ have the same shape as the point lattice function $\alpha_A^{PL}(R)$ so that the "shifted point lattice model" is quantitatively accurate in its predictions for both the polarizabilities and their distance derivatives.

The in-crystal polarizabilities computed for the 6-fold coordinated phase have been fitted to the light scattering model[33] both in its simplest form (4.3) introducing only the nearest cation neighbors but also in that (4.4) considering also the closest anion neighbors. Although only the latter provides a good description of the ab initio data, it must be concluded that this almost always arises solely from the introduction of two further fitting parameters and not because it introduces any significant physical effects absent from the nearest neighbor only description. Thus, the parameters emerging from using (4.4) predict that the second nearest neighbor anion−anion terms play a role comparable to that of the closest cation neighbors in reducing the anion polarizability. This contradicts the results of ab initio computations, which show that essentially the entire reduction of the in-crystal anion polarizabilities from the their free anion values is caused by just the nearest cation neighbors. We have suggested that the light scattering model would be guaranteed to yield parameters truly reflecting the physics of the in-crystal anion environment if these were determined by fitting to the results of two, rather than a single, series of ab initio computations. It has been shown that the light scattering model, with parameters determined from just the one series of ab initio computations presented here, provides a semiquantitatively accurate description of the anion polarizabilities in the phases having the zinc blende or cesium chloride structures.

Acknowledgment. E.B. thanks the Royal Society for a U.K. Relocation Fellowship. We thank both The Newton Trust (Cambridge University) and the Leverhulme Trust Foundation for financial support. We acknowledge the EPSRC National Service for Computational Chemistry Software for the provision of CPU time and access to the Q-Chem software.

Appendix 1

Computational Methods. *A1.1. Cation Basis Sets.* The basis set used for the Na^+ ion was the (10s9p) → [2s1p] contraction as previously constructed[30] where the primitive set was generated by deleting both all of the d functions and the most diffuse and the two most contracted s functions from the 13s9p5d set.[61] The three contracted functions are the closest approximations to the free ion Hartree−Fock orbitals constructable using this basis. The polarizability predicted for the free cation using this basis is exactly zero. However, in the CLUS computations, small but nonvanishing values arise through basis superposition error caused by the presence of the extended anion basis.

The primitives of s and p symmetry in the (10s9p3d) → [3s2p1d] basis set used for the K^+ ion were generated by deleting the most diffuse and the three most contracted s functions from the 14s9p set.[62] The three d functions are an even tempered set with exponents 3ζ, ζ, and $\zeta/3$ with ζ chosen to be 0.48 because this function attains its maximum at the same distance (1.4 a.u) as the mean radius of the potassium 3p orbital.[63] The contracted s and p functions are the closest approximations to the free ion Hartree−Fock orbitals constructable with this basis, whereas the contracted d function is that which reproduces the polarizability yielded by a [3s2p3d] basis consisting of the three contracted s and p functions plus the three d functions used uncontracted. The contracted [3s2p1d] set therefore reproduces that contribution to the polarizability which arises from the mixing of d symmetry components into the occupied orbitals of the free ion.

A1.2. Iodide Basis Set. The basis set for the iodide ion was chosen from the results of CLUS computations performed for NaI at its experimental equilibrium geometry of 3.238 Å[52] using the [2s1p] contracted set for the cation. Since the contribution of each of the six cations to the CLUS polarizability is only about 0.1 a.u., as shown below, one criterion for a satisfactory set is that it reproduces the experimental anion polarizability of 41.85 a.u. All of the polarizabilities were derived from "finite field computations" in which terms describing the interaction with a uniform electric field of strength 0.005 a.u. were added to the Hamiltonian. There are two different ways of deriving the polarizability. In the first of these, the polarizability is calculated by dividing the predicted dipole moment by the 0.005 a.u. strength (*F*) of the perturbing field. The second polarizability value, α^E, is calculated as $2(E_{nF} - E_F)/F^2$, where E_{nF} and E_F are the respective energies predicted in the absence and presence of the perturbing field. For the field independent basis sets used here, both methods yield the same results when implemented at the SCF level but differ when correlation is introduced using second-order Moller−Plesset perturbation theory.[64] All of the polarizabilities (α^{MPE}) at the second-order Moller−Plesset level were derived from the energies.

The results presented in Table A1 for the two standard basis sets,[65] the 6-311G* and the DeMon Coulomb Fitting (DeMon),

TABLE A1: Tests of Iodide Basis Sets for Anion in NaI at Experimental Separation (a.u.)[a]

basis	E_{HF}	α^{E}	α^{MPE}	basis	E_{HF}	α_{E}	α^{MPE}
6-311G*	−6916.90010	19.71	18.73				
DeMon	−6652.45805	34.82	32.59	DeMon+4f	−6652.45805	34.83	34.08
Trial	−6738.24241	41.05		Trial+4f	−6738.24241	41.26	
Huzinaga+	−6913.02362	41.24	41.87	Huzinaga+4f	−6913.02362	41.55	42.50

[a] E_{HF} Hartree−Fock energy of free iodide ion in absence of external electric field. α^{E} CHF polarizability. α^{MPE} Polarizability derived from differences between the field free and field present second-order Moller−Plesset energies.

show that neither of these sets, although useful within the contexts for which they were constructed, performs satisfactorily for the polarizability. Thus, the polarizabilities yielded by the 6-311G* set are far too small, whereas those predicted using the DeMon basis, although more reasonable, are still significantly too small. The predicted polarizabilities remain virtually unchanged when the DeMon set is augmented by four f functions having exponents equal to those of the four least contracted d functions to produce the set labeled DeMon+4f in Table A1.

Since the standard basis sets so far considered appeared to lack the diffuse functions needed to describe fully the polarizability, a new basis set, labeled Trial, (Table A1) was constructed. The s functions consisted of the those in the DeMon basis, which is an even tempered set having an exponent ratio (r) of 1/5, augmented by the next more diffuse functions generated by extending this even tempered sequence. The set of seven p functions consisted of an even tempered sequence of five functions having the same r of 1/5 constructed by demanding that one member of this set had $\zeta = 0.08$ so that its maximum coincided with the mean radius (2.5 a.u.[63]) of the iodine 5p Hartree−Fock orbital, whereas another member ($\zeta = 50.0$) had its maximum at the mean radius of the Hartree−Fock 2p orbital. The final two functions had exponents of 150 and 0.016. The even tempered set of seven d functions with $r = 1/3$, with most contracted member having $\zeta = 32.4$, was constructed by demanding that one member ($\zeta = 1.2$) reaches its maximum at a distance (0.91 a.u.) equal to the mean radius of the iodine Hartree−Fock 4d orbital.[63] The Trial+4f set was constructed by augmenting the Trial basis with an even tempered sequence of four f functions having $r = 1/3$ with exponents chosen such that each function attained its maximum value at the same distance as that at which the corresponding d function was a maximum. This produced a ζ value of 1.8 for the most contracted member of this set. The polarizabilities (Table A1) predicted using either the Trial or the Trial+4f bases are entirely satisfactory, which indicates that many of the difficulties with the previously considered sets arose from their lack of polarization functions. Nevertheless, nether of these two bases can be considered to be entirely satisfactory because the energy of −6738.24241 a.u. predicted for the total Hartree−Fock energy of the free iodide ion, although much lower than those derived from the previous basis sets, is still significantly greater than either that of −6918.06366 a.u. yielded by the Clementi and Roetti[66] Slater basis or the numerical Hartree−Fock value of −6918.07614 a.u.[63]

The (21s16p10d4f) → [10s7p5d4f] basis finally adopted for all of the computations reported in the main body of the paper, that labeled Huzinaga+4f in Table A1, was constructed by augmenting the (16s13p7d) → [5s3p2d] basis of Huzinaga,[67] which yields an acceptable total energy, with the additional diffuse functions from the Trail+4f set needed to describe the polarizability. The five additional s functions were an even-tempered set with $r = 1/3$ with the most contracted function having $\zeta = 1$. The three additional p basis functions are an even-tempered set with $r = 1/3$ with the most contracted function having $\zeta = 0.1$. The four f functions and the three additional d functions are the most diffuse members from the Trail+4f basis. The basis labeled Huzinaga+ differs from the Huzinaga+4f set only in the absence of the f functions. For the free iodide ion, the total energy of −6912.950448 a.u. predicted with the QCHEM program using the original Huzinaga basis agrees with the literature value of −6912.95043 a.u.[66] The Huzinaga+ and Huzinaga+4f sets not only predict a lower total energy than the original Huzinaga set but also yield entirely satisfactory predictions for the anion polarizability in NaI.

A1.3. Basis Superposition Corrections. The cation description in a cluster is modified through the availability of anion basis functions. Consequently, each computed cluster polarizability α_{CLUS} contains cation polarizability contributions, which are absent from the value computed for an isolated cation using the basis sets presented above in section A1.1. The previous approach[30] was to use contracted [2s1p] and [3s2p] bases for Na^+ and K^+, respectively, providing a near Hartree−Fock quality description of the free ions. The basis superposition correction to be subtracted from α_{CLUS} was derived by computing the polarizability of the cluster of n_{CA} cations in the presence of either all of the anion basis functions or, alternatively, a subset. The subset was constructed by deleting functions contributing little to the cation polarizability in the full computation by virtue of describing the occupied anion orbitals. For sodium salts, this approach works well[23,29−32] with the computed superposition corrections being no more than 0.15 a.u. per cation[30] even when all of the anion basis functions are included in the counterpoise computation. The small size of these corrections not only means that the dipole−induced dipole terms will be very small but also that the second approach of including only a subset of the anion basis functions will predict even smaller cation superposition corrections. Thus, the uncertainties in the predicted anion polarizabilities are almost insignificant. However, for potassium salts, this approach was not satisfactory with uncertainties between 4 a.u and 6 a.u. in the predicted the anion polarizabilities.[30] The true polarizability of K^+ is five times greater than that for Na^+; the superposition corrections are as large as 1 a.u. per cation if all of the anion basis functions are included. This not only means that significant ambiguities in the choice of anion functions to be included in the computation of the superposition corrections will be propagated into the final predictions of the anion polarizabilities but also that the dipole induced dipole contributions in the cluster should not be neglected.

The difficulties just discussed were circumvented in the present work by computing at each R the polarizability attained by one cation in the cluster. This computed α_C is then used in eq 2.1 for all three polymorphs to derive α_A from the three different phase dependent α_{CLUS}. This required polarizability of a single cation was computed using a basis in which the appropriate contracted cation set described in section A1.1 is augmented with all but one of the additional polarization functions, located at the position of the anion nucleus, present in the (21s16p10d4f) → [10s7p5d4f] iodide basis. The [5s3p2d] contracted functions in the original Huzinaga set are discarded

TABLE A2: Experimental Data Used to Derive the Anion Polarizability Distance Derivatives[a]

LiF

variables	p_{11}	$p_{11}-p_{12}$	p_{11}	p_{12}	$(R/\epsilon_\infty)\mathrm{d}\epsilon_\infty/\mathrm{d}R$	$\rho(\mathrm{d}n/\mathrm{d}\rho)$	$\mathrm{d}n/\mathrm{d}P$	K^{-1}
data	0.02	-0.108	0.02	0.13	-0.57	0.13	0.198	0.67
ref	68		69		70	71	72	
$[V\mathrm{d}\epsilon_\infty/\mathrm{d}V]_{V=V_e}$	-0.3413		-0.3462		-0.3659	-0.3608	-0.3682	
$[\mathrm{d}\alpha_A/\mathrm{d}R]_{R=R_e}$	3.498		3.478		3.399	3.485	3.390	

variables	Λ_0	α_m	Λ_0	α_m	$\rho(\mathrm{d}n/\mathrm{d}\rho)$	
data	0.719	0.915	0.65	0.915	0.125	
ref	73	52	74	52	58	75
$[V\mathrm{d}\epsilon_\infty/\mathrm{d}V]_{V=V_e}$					-0.3469	-0.40
$[\mathrm{d}\alpha_A/\mathrm{d}R]_{R=R_e}$	3.508		3.172		3.475	3.262

NaF

variables	$\rho(\mathrm{d}n/\mathrm{d}\rho)$	$\mathrm{d}n/\mathrm{d}P$	B	p_{11}	p_{12}	$\mathrm{d}n/\mathrm{d}P$	K^{-1}		$\rho(\mathrm{d}n/\mathrm{d}\rho)$
data	0.11	0.272	0.465	0.02	0.13	0.398	0.465		0.124
ref	71	60	76	77		72	75	78	
$[V\mathrm{d}\epsilon_\infty/\mathrm{d}V]_{V=V_e}$	-0.2906	-0.3342		-0.1218		-0.4889	-0.33	-0.3276	
$[\mathrm{d}\alpha_A/\mathrm{d}R]_{R=R_e}$	3.756	3.500		4.748		2.591	3.525	3.539	

NaCl

variables	p_{11}	$p_{11}-p_{12}$	$(R/\epsilon_\infty)\mathrm{d}\epsilon_\infty/\mathrm{d}R$	$\rho(\mathrm{d}n/\mathrm{d}\rho)$	$\mathrm{d}n/\mathrm{d}P$	K^{-1}	p_{11}	p_{12}	
data	0.11	-0.043	-0.95	0.28	1.170	0.24	0.115	0.161	
ref	68		70	71	60	76	79		75
$[V\mathrm{d}\epsilon_\infty/\mathrm{d}V]_{V=V_e}$	-0.7555		-0.7392	-0.8556	-0.8580		-0.7936		-0.85
$[\mathrm{d}\alpha_A/\mathrm{d}R]_{R=R_e}$	7.359		7.359	6.730	6.715		7.119		6.765

	NaCl		NaBr				NaI	RbI	
variables	$\rho(\mathrm{d}n/\mathrm{d}\rho)$			$\mathrm{d}n/\mathrm{d}P$	K^{-1}	$\rho(\mathrm{d}n/\mathrm{d}\rho)$	$\rho(\mathrm{d}n/\mathrm{d}\rho)$	$\mathrm{d}n/\mathrm{d}P$	K^{-1}
data	0.268	0.276		1.570	0.2	0.360	0.490	4.25	0.106
ref	58	78	75	72		78	58	72	
$[V\mathrm{d}\epsilon_\infty/\mathrm{d}V]_{V=V_e}$	-0.8189	-0.8433	-0.99	-1.0127		-1.1611	-1.6959	-1.446	
$[\mathrm{d}\alpha_A/\mathrm{d}R]_{R=R_e}$	6.961	6.807	9.467	9.321		8.361	10.473	9.24	

KI

variables	p_{11}	$p_{11}-p_{12}$	$(R/\epsilon_\infty)\mathrm{d}\epsilon_\infty/\mathrm{d}R$	$\rho(\mathrm{d}n/\mathrm{d}\rho)$		p_{11}	p_{12}	$\mathrm{d}n/\mathrm{d}P$	K^{-1}	
data	0.21	0.041	-1.57	0.438	0.44	0.208	0.166	3.85	0.117	
ref	68		70	80	71	79		72		75
$[V\mathrm{d}\epsilon_\infty/\mathrm{d}V]_{V=V_e}$	-1.282		-1.386	-1.426	-1.4322	-1.2629		-1.4622		-1.28
$[\mathrm{d}\alpha_A/\mathrm{d}R]_{R=R_e}$	11.821		10.359	10.004	9.949	11.450		9.648		11.298

[a] $\mathrm{d}n/\mathrm{d}P$ in 10^{-12} cm^2 dyne^{-1}, B and K^{-1} in 10^{12} dyne cm^{-2}, α_m in Å^3, and $[\mathrm{d}\alpha_A/\mathrm{d}R]_{R=R_e}$ in a.u. In columns not containing a variable heading, $[V\mathrm{d}\epsilon_\infty/\mathrm{d}V]_{V=V_e}$ is directly reported in the indicated reference.

because these constitute near Hartree−Fock quality orbitals occupied by the anion electrons, whereas the s primitive having $\zeta = 1.0$ is more contracted than the most diffuse s member of the Huzinaga set. The electric field is applied along the x direction perpendicular to the z axis joining the positions of the cation and anion nuclei. This geometry corresponds to the positions of four of the six cations in a full cluster. There is no x component of the dipole in the absence of the field, and so the total energy in the presence of the field is just the sum of the field free energy and the second order correction $-\alpha_C F^2/2$. Hence, both CHF and MPE values for α_C can be deduced from the energies because no knowledge of the induced dipole moment is required. However, since this system has a nonvanishing z dipole in the absence of the field, the total energy in the presence of a field applied along the z direction contains additionally the first-order energy of interaction between the field and the unperturbed z dipole. Consequently, it was not possible to derive MP2 values for this counterpoise corrected cation polarizability. However, SCF values for α_C could be derived, the value of 6.59 a.u. for K^+ at $R = 6.676$ a.u., when the field is applied along the z-direction being similar to that of 6.23 a.u. for the field applied in the x direction.

For Na^+, the corrections are very small; for example, for the 6:6 NaI polymorph at its experimental equilibrium geometry, the MPE a_C computed using the perpendicularly applied (x) field is a mere 0.10 a.u.; consequently the computed α_{CLUS} of 42.50 a.u is only slightly greater than the 41.82 a.u. value of α_A (Table 1) derived from (2.1). However, the KI calculations show the necessity for the present approach because the a_C computed with the inclusion of these diffuse anion basis functions are large. For example, for the 6:6 phase at equilibrium, the a_C computed at the CHF and MPE levels are 6.23 and 6.53 a.u., respectively, with corresponding α_{CLUS} values of 80.60 and 83.42 a.u.

Appendix 2

Experimental Data Needed for the Derivation of the Anion Polarizability Derivatives. The quantity $[V\mathrm{d}\epsilon_\infty/\mathrm{d}V]_{V=V_e}$ needed to derive $[\mathrm{d}\alpha_A/\mathrm{d}R]_{R=R_e}$ can be derived from four different types of experiment in addition to those determining the former quantity directly. First, measurements of the density (ρ) dependence of the refractive index (n_∞) in the form $\rho\mathrm{d}n/\mathrm{d}\rho$ yields $[V\mathrm{d}\epsilon_\infty/\mathrm{d}V]_{V=V_e}$ through the relation

$$[V\mathrm{d}\epsilon_\infty/\mathrm{d}V]_{V=V_e} = -2n_\infty(\rho\mathrm{d}n/\mathrm{d}\rho) \quad \text{(A2.1)}$$

which follows directly after noting that $\epsilon_\infty = n_\infty^2$. Second, $\rho\mathrm{d}n/\mathrm{d}\rho$ can be derived from measurements of the optical strain coefficients p_{11} and p_{12} through the relation[68]

$$\rho\mathrm{d}n/\mathrm{d}\rho = (n_\infty^3/6)(p_{11} + 2p_{12}) \quad \text{(A2.2)}$$

and the resulting values substituted into (A2.1). Third, values of $[V\mathrm{d}\epsilon_\infty/\mathrm{d}V]_{V=V_e}$ can be derived by combining measured values of the pressure dependence $\mathrm{d}n/\mathrm{d}P$ of the refractive index with those of the bulk modules (B) equal to the inverse of the compressibility (K). Since all of the measurements and mathematical manipulations refer to a constant temperature, the constant temperature condition on the derivatives need not be explicitly indicated. Since there is only one independent variable which can be chosen to be either the pressure or volume, it follows that one can write

$$\mathrm{d}n/\mathrm{d}P = (\mathrm{d}n/\mathrm{d}V)\,(\mathrm{d}V/\mathrm{d}P) \quad \text{(A2.3)}$$

Introducing the definition of the bulk modulus

$$B = K^{-1} = -V(\mathrm{d}p/\mathrm{d}V) \quad \text{(A2.4)}$$

it follows that

$$\mathrm{d}n/\mathrm{d}V = -(B/V)(\mathrm{d}n/\mathrm{d}P) \quad \text{(A2.5)}$$

Introduction of the relation $V\mathrm{d}\epsilon/\mathrm{d}V = -2nV(\mathrm{d}n/\mathrm{d}V)$ yields the desired result

$$[V\mathrm{d}\epsilon_\infty/\mathrm{d}V]_{V=V_e} = -2n_\infty B(\mathrm{d}n/\mathrm{d}P) \quad \text{(A2.6)}$$

The fourth experimental quantity for which values are available is $(R_e/\epsilon_\infty)(\mathrm{d}\epsilon_\infty/\mathrm{d}R)_{R=R_e}$. Noting that $V = 2R^3$ for B1 structured crystals, it follows that

$$[V\mathrm{d}\epsilon_\infty/\mathrm{d}V]_{V=V_e} = (\epsilon_\infty/3)[(R_e/\epsilon_\infty)(\mathrm{d}\epsilon_\infty/\mathrm{d}R)_{R=R_e}] \quad \text{(A2.7)}$$

Finally, experimental values are available for the Muller parameter Λ_0 from which $[\mathrm{d}\alpha_A/\mathrm{d}R]_{R=R_e}$ can be derived through the relation[29]

$$[\mathrm{d}\alpha_A/\mathrm{d}R]_{R=R_e} = 3\alpha_m\Lambda_0/R_e \quad \text{(A2.8)}$$

The data needed to evaluate either $[V\mathrm{d}\epsilon_\infty/\mathrm{d}V]_{V=V_e}$ or $[\mathrm{d}\alpha_A/\mathrm{d}R]_{R=R_e}$ directly from (3.2) are presented in Table A2.The only other variables entering the right-hand sides of (A2.1), (A2.2), (A2.6), (A2.7), and (A2.8) are n_∞, ϵ_∞, and R_e. The values of the former used are presented in Table 5, ϵ_∞ being calculated as n_∞^2, whereas the distances R_e are taken from Table 1. Similarly the values of $[\mathrm{d}\alpha_A/\mathrm{d}R]_{R=R_e}$ were calculated from (3.2) using the same data set for both ϵ_∞ and R_e.

The anion polarizabilities computed ab initio are related through the relations (A2.1) to (A2.8) and (3.2) to the refractive indices and high-frequency dielectric constants extrapolated to infinite wavelength. However, the experimental values for $\rho(\mathrm{d}n/\mathrm{d}\rho)$, p_{11}, p_{12}, $\mathrm{d}n/\mathrm{d}P$, and Λ_0 were measured at finite wavelength. Since it should be expected that these would differ only slightly from their extrapolated counterparts, the former should be regarded as the best available approximations to the latter. This justifies using the extrapolated values for n_∞ presented in Table 1. In particular, the fourth power of n_∞ arises when $[V\mathrm{d}\epsilon_\infty/\mathrm{d}V]_{V=V_e}$ is calculated from $\rho(\mathrm{d}n/\mathrm{d}\rho)$ using (A2.2) followed by (A2.1). The use of the larger non-extrapolated values for the refractive index would therefore yield less accurate values for $[V\mathrm{d}\epsilon_\infty/\mathrm{d}V]_{V=V_e}$ and hence for $[\mathrm{d}\alpha_A/\mathrm{d}R]_{R=R_e}$.

References and Notes

(1) Pyper, N. C. *Adv. Solid State Chem*. **1991**, *2*, 223−393.
(2) Madden, P. A.; Wilson, M. *Chem. Soc. Rev*. **1996**, *25*, 339−350.
(3) Mayer, J. E. *J. Chem. Phys*. **1933**, *1*, 270−279.
(4) Mott, N. F.; Gurney, R. W. *Electronic Processes in Ionic Crystals*; Oxford University Press: Oxford, U.K., 1950.
(5) Herzfeld, K. F. *Phys. Rev*. **1927**, *29*, 701−705.
(6) Edwards, P. P.; Sienko, M. J. *Int. Rev. Phys. Chem*. **1983**, *3*, 83−144.
(7) Ross, M. *J. Chem. Phys*. **1972**, *56*, 4651−4653.
(8) Mavroyannis, C.; Stephen, M. J. *Mol. Phys*. **1962**, *5*, 629−638.
(9) McLachlan, A. D. *Proc. R. Soc. A* **1963**, *271*, 387−401.
(10) Slater, J. C.; Kirkwood, J. G. *Phys. Rev*. **1931**, *37*, 682−697.
(11) Tang, K. T. *Phys. Rev*. **1969**, *177*, 108−114.
(12) May, A. *Phys. Rev*. **1937**, *52*, 339−347.
(13) May, A. *Phys. Rev*. **1938**, *54*, 629−633.
(14) Pyper, N. C. *Phil. Trans. R. Soc. A* **1986**, *320*, 107−158.
(15) Pyper, N. C. *Phil. Trans. R. Soc. A* **1995**, *352*, 89−123.
(16) Pyper, N. C. *Chem. Phys. Lett*. **1994**, *220*, 70−76.
(17) Pyper, N. C. *J. Chem. Phys*. **2003**, *118*, 2308−2324.
(18) Pyper, N. C.; Kirkland, A. I.; Harding, J. H. *J. Phys. Condens. Matter* **2006**, *18*, 683−702.
(19) Mott, N. F.; Littleton, M. J. *Trans. Faraday Soc*. **1938**, *34*, 485−499.
(20) Harding, J. H. *Rep. Prog. Phys*. **1991**, *53*, 1403−1466.
(21) Wilson, M.; Madden, P. A. *J. Phys. Condens. Matter* **1994**, *6*, 159−170.
(22) Fowler, P. W.; Madden, P. A. *Mol. Phys*. **1983**, *49*, 913−923.
(23) Fowler, P. W.; Madden, P. A. *Phys. Rev. B* **1984**, *29*, 1035−1042.
(24) Fowler, P. W.; Madden, P. A. *J. Phys. Chem. B* **1985**, *89*, 2581−2585.
(25) Fowler, P. W.; Pyper, N. C. *Proc. R. Soc. A* **1985**, *398*, 377−393.
(26) Fowler, P. W.; Knowles, P. J.; Pyper, N. C. *Mol. Phys*. **1985**, *56*, 83−95.
(27) Fowler, P. W.; Tole, P. *J. Chem. Soc. Faraday Trans*. **1990**, *86*, 1019−1023.
(28) Pyper, N. C. *Mol. Phys*. **1998**, *95*, 1−15.
(29) Jemmer, P.; Fowler, P. W.; Wilson, M.; Madden, P. A. *J. Phys. Chem. A* **1998**, *102*, 8377−8385.
(30) Pyper, N. C.; Popelier, P. *J. Phys. Condens. Matter* **1997**, *9*, 471−488.
(31) Fowler, P. W.; Tole, P. *Chem. Phys. Lett*. **1990**, *149*, 273−277.
(32) Wilson, M.; Madden, P. A.; Jemmer, P.; Fowler, P. W.; Batana, A.; Bruno, J.; Munn, R. W.; Monrad, M. C. *Mol. Phys*. **1998**, *96*, 1457−1467.
(33) Madden, P. A.; O'Sullivan, K.; Board, J. A.; Fowler, P. W. *J. Chem. Phys*. **1991**, *94*, 918−927.
(34) Meyer, R. R.; Sloan, J.; Dunin-Borkowski, R. E.; Kirkland, A. I.; Novotny, M. C.; Bailey, S. R.; Hutchinson, J. L.; Green, M. L. H. *Science* **2000**, *289*, 1324−1326.
(35) Sloan, J.; Novotny, M. C.; Bailey, S. R.; Brown, G.; Xu, C.; Williams, V. C.; Friedrichs, S.; Flahaut, E.; Callender, R. L.; York, A. P. E.; Coleman, K. S.; Green, M. L. H.; Dunin-Borkowski, R. E.; Hutchinson, J. L. *Chem. Phys. Lett*. **2000**, *329*, 61−65.
(36) Sloan, J.; Friedrichs, S.; Meyer, R. R.; Kirkland, A. I.; Hutchison, J. L.; Green, M. L. H. *Inorg. Chim. Acta* **2002**, *330*, 1−12.
(37) Sloan, J.; Kirkland, A. I.; Hutchison, J. L.; Green, M. L. H. *Comptes Rendu* **2003**, *4* (part 9) 1063−1074.
(38) Philip, E.; Sloan, J.; Kirkland, A. I.; Meyer, R. R.; Friedrichs, S.; Hutchison, J. L.; Green, M. L. H. *Nat. Mater*. **2003**, *2*, 778−791.
(39) Sloan, J.; Kirkland, A. I.; Hutchison, J. L.; Green, M. L. H. *Chem. Comm*. **2002**, 1319−1332.
(40) Wilson, M.; Madden, P. A. *J. Am. Chem. Soc*. **2001**, *123*, 2101−2102.
(41) Wilson, M. J. *J. Chem. Phys*. **2002**, *116*, 3027−3041.
(42) Bichoutskaia, E.; Pyper, N. C. *J. Phys. Chem. B* **2006**, *110*, 5936−5949.
(43) Bichoutskaia, E.; Pyper, N. C. *Chem. Phys. Lett*. **2006**, *423*, 234−239.
(44) Kirkland, A. I.; Saxton, W. O.; Chand, G. *J. Electron Microsc*. **1997**, *46*, 11−22.
(45) Meyer, R. R.; Kirkland, A. I.; Saxton, W. O. *Ultramicroscopy* **2002**, *92*, 89−109.
(46) Mahan, G. D. *Solid State Ionics* **1980**, *1*, 29−45.
(47) Fowler, P. W. *Mol. Simul*. **1990**, *4*, 313−330.
(48) Q-Chem 2.0: A high-performance ab initio electronic structure program; Kong, J.; White, C. A.; Krylov, A. I.; Sherrill, C. D.; Adamson, R. D.; Furlani, T. R.; Lee, M. S.; Lee, A. M.; Gwaltney, S. R.; Adams, T. R.; Ochsenfeld, C.; Gilbert, A. T. B.; Kedziora, G. S.; Rassolov, V. A.;

Maurice, D. R.; Nair, N.; Shao, Y.; Besley, N. A.; Maslen, P. E.; Dombroski, J. P.; Daschel, H.; Zhang,W.; Korambath, P. P.; Baker J.; Byrd, E. F. C.; Van Voorhis, T.; Oumi, M.; Hirata, S.; Hsu, C.-P.; Ishikawa, N.; Florian, J.; Warshel, A.; Johnson, B. G.; Gill, P. M. W.; Head-Gordon, M.; Pople, J. A. *J. Comput. Chem.* **2000**, *21*, 1532−1548.

(49) McEachran, R. P.; Stauffer, A. D.; Greita, S. *J. Phys. B* **1979**, *12*, 3119−3123.

(50) Johnson, W. R.; Kolb, D.; Huang, K. N. *At. Data Nucl. Data Tables* **1983**, *28*, 333−340.

(51) Rose, S. J.; Grant, I. P.; Pyper, N. C. *J. Phys. B* **1979**, *11*, 1171−1176.

(52) Wilson, J. N.; Curtis, R. M. *J. Phys. Chem*. **1970**, *74*, 187−196.

(53) Landolt-Bornstein, Z. *Series III*; Hellwege, K. H., Hellwege, A. M., Eds.; Springer-Verlag: Berlin, 1973.

(54) Dierckson, G. H. F.; Sadlej, A. J. *Mol. Phys*. **1982**, *47*, 33−53.

(55) Dierckson, G. H. F.; Sadlej, A. J. *Chem. Phys. Lett*. **1981**, *84*, 390−396.

(56) Kello, V.; Roos, B. O.; Sadlej, A. J. *Theor. Chim. Acta* **1988**, *74*, 185−194.

(57) Nellin, C.; Roos, B. J.; Sadlej, A. J.; Seigbahn, P. E. M. *J. Chem. Phys*. **1982**, *77*, 3607−3614.

(58) Johannsen, P. G. *Phys. Rev. B* **1997**, *55*, 6856−6864.

(59) Shanker, J.; Agrawal, G. G.; Singh, R. P. *Philos. Mag. B* **1979**, *39*, 405−411.

(60) Fontanella, J.; Andeen, C.; Schuele, D. *Phys. Rev. B* **1972**, *6*, 582−590.

(61) Dierckson, G. H. F.; Sadlej, A. J. *Theor. Chim. Acta* **1982**, *61*, 485−504.

(62) Watchers, A. J. H. *J. Chem. Phys*. **1970**, *52*, 1033−1036.

(63) Froese-Fischer, C. *At. Data*, **1972**, *4*, 301−399.

(64) Amos, R. D. *Chem. Phys. Lett*. **1982**, *88*, 89−94.

(65) Basis sets were obtained from the Extensible Computational Chemistry Environment Basis Set Database, version 4/05/02, as developed and distributed by the Molecular Science Computing Facility, Environmental and Molecular Sciences Laboratory which is part of the Pacific Northwest Laboratory, P.O. Box 999, Richland, Washington 99352, U.S.A., and funded by the U.S. Department of Energy. The Pacific Northwest Laboratory is a multi- program laboratory operated by Battelle Memorial Institute for the U.S. Department of Energy under contract DE-AC06−76RLO 1830. Contact David Feller or Karen Schuchardt for further information.

(66) Clementi, E.; Roetti, C. *At. Data Nucl. Data Tables* **1974**, *14*, 177−196.

(67) Huzinaga, S. *Gaussian basis sets for molecular calculations, Physical Sciences data 16*; Elsevier: Amsterdam, 1984.

(68) Burnstein, E.; Smith, P. L. *Phys. Rev*. **1948**, *74*, 229−230.

(69) Iyengar, K. S. *Nature* **1955**, *176*, 1119−1120.

(70) Van Vecthen, J. A. *Phys. Rev*. **1969**, *182*, 891−905.

(71) Waxler, R. M. *IEEE J. Quantum Electron*. **1971**, *7*, 166−167.

(72) Bendow, B.; Gianino, P. D.; Tsay, Y. F.; Mitra, S. S. *Appl. Opt*. **1974**, *13*, 2382−2396.

(73) Coker, H. *J. Phys. Chem. Solids* **1979**, *40*, 1079−1088.

(74) Balzaretti, N. M.; Da, Jornada, J. A. H. *J. Phys. Chem. Solids* **1996**, *57*, 179−182.

(75) Singh, A. V.; Sharma, J. C.; Shanker, J. *Physica B* **1978**, *94*, 331−345.

(76) Tsay, Y. T.; Bendow, B.; Mitra, S. S. *Phys. Rev. B* **1973**, *8*, 2688−2696.

(77) Pohl, D. W.; Schwarz, S. E. *Phys. Rev. B* **1973**, *7*, 2735−2739.

(78) Johannsen, P. G.; Reiss, G.; Bohle, U.; Magiera, J.; Muller, R.; Spiekermann, H.; Holzapfel, W. B. *Phys. Rev. B* **1997**, *55*, 6865−6870.

(79) Benckert, L.; Backstrom, G. *Phys. Rev. B* **1973**, *8*, 5888−5893.

(80) Vedam, K.; Schmidt, E. D. D.; Kirk, J. L.; Schneider, W. C. *Mater. Res. Bull*. **1969**, *4*, 573−580.